Eur. Phys. J. B **48**, 29–36 (2005)
DOI: 10.1140/epjb/e2005-00380-3

THE EUROPEAN PHYSICAL JOURNAL B

Omnidirectional reflection from the one-dimensional photonic crystal containing anisotropic left-handed material

S. Wang[1,a] and L. Gao[2,1]

[1] Department of Physics, Suzhou University, Suzhou 215006, P.R. China
[2] CCAST (World Laboratory), P.O. Box 8730, Beijing 100080, P.R. China

Received 27 June 2005 / Received in final form 5 August 2005
Published online 9 December 2005 –

Abstract. We study the transmission properties in the one-dimensional photonic crystal containing alternate anisotropic left-handed material (LHM) layers and regular isotropic right-handed material (RHM) layers. For such an anisotropic case, the dispersion relation from the Bloch theorem is derived and the Bragg gaps of the periodic structure are observed. It is found that in the $m = 0$ Bragg gap, there is an omnidirectionally reflectional (ODR) region, which is also invariant with a change of scale length, similar with the $\bar{n} = 0$ gap in isotropic one-dimensional photonic crystal. With the aid of effective medium theory (EMT), the analytic expressions of all six elements of the effective electric permittivity tensor and magnetic permeability tensor are obtained. By using these results, we investigate the ODR region in the $m = 0$ Bragg gap in all the possible cases of both TE and TM modes. We find that with different choices of parameters, the $m = 0$ Bragg gap has different transmission properties, and the ODR region in it changes, consequently. The edges of the ODR region are given out in these cases. To one's interest, these results predict a complete reflection region in the $m = 0$ Bragg gap, which is able to omnidirectionally reflect waves in both TE and TM modes.

PACS. 02.30.Mv Approximations and expansions – 42.25.-p Wave optics – 42.70.Qs Photonic bandgap materials – 78.20.Ci Optical constants (including refractive index, complex dielectric constant, absorption, reflection and transmission coefficients, emissivity)

1 Introduction

During the recent years, considerable experimental and theoretical efforts have been devoted to the study of a new kind of metamaterials that have simultaneously negative electric permittivity ε and magnetic permeability μ. These metamaterials are termed as "left-handed materials" due to the fact that the electric field vector $\mathbf{E}$, the magnetic field vector $\mathbf{H}$ and the wave vector $\mathbf{k}$ form a left-handed triplet other than that in the conventional materials [1], and they can be experimentally realized by repetition of arrays of split ring resonator and wires [2,3]. This kind of materials have many unique properties such as the reversal of Doppler shift for radiation, the reversal of Cerenkov radiation and the famous negative refraction. Recently, Pendry predicted that a slab of this left-handed material with ε, $\mu = -1$ can theoretically make a perfect lens [4]. However, whether this perfect lens can be realized in practice is still controversial [5,6].

Omnidirectional reflectors have attracted significant attention in the last few years. The omnidirectional reflection obtained from one-dimensional photonic crystal has been reported since 1998 [7–10]. Recent reports showed that the one-dimensional photonic crystal consists of LHM and RHM can present a special band gap, corresponding to that the average index equals to zero, i.e., $\bar{n} = 0$. This gap not only can reflect waves with all incident angles, but also won't change when the structure undergoes scaling [11,12]. Further research showed that the one-dimensional quasiperiodic structure consists of LHM and RHM also possesses the $\bar{n} = 0$ gap [13]. In all the content mentioned above, the materials involved are all isotropic, however, the anisotropic materials can also obtain omnidirectional reflection. The one-dimensional photonic crystal formed by alternate anisotropic RHM layers where the optic axis direction of the layers rocks back and forth around the normal to the layers' surfaces can also make an omnidirectional reflector [14,15]. Since the LHM realized in the experiments are always anisotropic and the negative refraction can be realized in the uniaxial metamaterials with only one or two elements of the permittivity tensor and permeability tensor is negative, it is necessary to consider the anisotropy of the LHM and the one-dimensional structure containing anisotropic LHM. Quite recently, Liu et al showed that a slab of uniaxially anisotropic LHM can make an omnidirectional

[a] e-mail: lgaophys@pub.sz.jsinfo.net

reflector [16]. In this paper, we are interested in the omnidirectional reflection obtained from the one-dimensional photonic crystal containing alternate anisotropic left-handed material and isotropic right-handed material. Using the Bloch theorem, we obtain the dispersion relation for this anisotropic case. To the best of our knowledge, the dispersion relation for such an infinite periodic anisotropic structure is first reported. Furthermore, with the aid of the EMT method, we investigate the $m = 0$ Bragg gap, and analyze the ODR region in it in all the possible cases of both TE and TM modes.

This paper is organized as follows: in Section 2, we describe the theoretical model of our system and derive the dispersion relation by using the Bloch theorem. Then, by using the EMT method, we obtain the analytic expressions of the elements of the effective electric permittivity and magnetic permeability tensors. In Section 3, the two different cases of TE mode wave are studied and the ODR region is found and quite well described with EMT. In Section 4, two different cases of TM mode are investigated. The discussion on the cases with other choice of parameters and the conclusion are given out in Section 5.

2 Theoretical development

We consider the one-dimensional photonic crystal consists of alternate anisotropic left-handed material layers and isotropic right-handed material layers embedded in vacuum. We choose the layers to be parallel to the x–y plane with the z-axis normal to the interfaces of the layers. To simplify the proceeding analysis, we assume the anisotropic LHM layers with the electric permittivity $\bar{\bar{\varepsilon}}_L$ tensor and magnetic permeability $\bar{\bar{\mu}}_L$ tensor to be simultaneously diagonalizable, i.e.,

$$\bar{\bar{\varepsilon}}_L = \begin{pmatrix} \varepsilon_{Lx} & 0 & 0 \\ 0 & \varepsilon_{Ly} & 0 \\ 0 & 0 & \varepsilon_{Lz} \end{pmatrix}, \quad \bar{\bar{\mu}}_L = \begin{pmatrix} \mu_{Lx} & 0 & 0 \\ 0 & \mu_{Ly} & 0 \\ 0 & 0 & \mu_{Lz} \end{pmatrix}. \quad (1)$$

2.1 Dispersion relation

For a TE mode case, the electric and magnetic fields in one unit cell can be expressed as [17],

$$\begin{aligned} E_{Ly} &= e^{ik_x x}\left(e^{ik_{Lz}z} + Ae^{-ik_{Lz}z}\right), \\ H_{Lx} &= \frac{-k_{Lz}}{\omega\mu_{Lx}} e^{ik_x x}\left(e^{ik_{Lz}z} - Ae^{-ik_{Lz}z}\right), \\ H_{Lz} &= \frac{k_x}{\omega\mu_{Lz}} e^{ik_x x}\left(e^{ik_{Lz}z} + Ae^{-ik_{Lz}z}\right), \end{aligned} \quad (2)$$

in anisotropic LHM layer and

$$\begin{aligned} E_{Ry} &= e^{ik_x x}\left(Be^{ik_{Rz}z} + Ce^{-ik_{Rz}z}\right), \\ H_{Rx} &= \frac{-k_{Rz}}{\omega\mu_{Rx}} e^{ik_x x}\left(Be^{ik_{Rz}z} - Ce^{-ik_{Rz}z}\right), \\ H_{Rz} &= \frac{k_x}{\omega\mu_{Rz}} e^{ik_x x}\left(Be^{ik_{Rz}z} + Ce^{-ik_{Rz}z}\right), \end{aligned} \quad (3)$$

in RHM layer, where k_{Lz} and k_{Rz} are the z-components of the wave vectors in the LHM and RHM layers, and k_x is the x-component. The differences between the electromagnetic waves in the LHM and RHM lie in the signs of permittivity ε and permeability μ, thus leads to different signs of k_{Lz} and k_{Rz}. The plane wave solutions specified by (2) and (3) yields the following equation for determining $k_{L,Rz}$,

$$k_{L,Rz}^2 = \varepsilon_{L,Ry}\mu_{L,Rx}\frac{\omega^2}{c^2} - \frac{\mu_{L,Rx}}{\mu_{L,Rz}}k_x^2. \quad (4)$$

The tangential electric and magnetic field should be continuous at the interface (let it to be $z = 0$), i.e.,

$$\begin{aligned} E_{Ly}(z = 0^-) &= E_{Ry}(z = 0^+), \\ H_{Lx}(z = 0^-) &= H_{Rx}(z = 0^+). \end{aligned} \quad (5)$$

In addition, since the system is periodic, the electric and magnetic field should obey the Bloch theorem, i.e.,

$$\begin{aligned} E_{Ly}(z = d_L) &= E_{Ry}(z = -d_R)e^{iqd}, \\ H_{Lx}(z = d_L) &= H_{Rx}(z = -d_R)e^{iqd}, \end{aligned} \quad (6)$$

where d_L, d_R are the thicknesses of single LHM and RHM layer, respectively, d is the thickness of a unit cell and q is the Bloch wave vector. The dispersion relation can be derived from all these relations,

$$\begin{aligned} \cos(qd) &= \cos\left(k_{Lz}d_L\right)\cos(k_{Rz}d_R) \\ &- \frac{1}{2}\left(\frac{\mu_{Rx}k_{Lz}}{\mu_{Lx}k_{Rz}} + \frac{\mu_{Lx}k_{Rz}}{\mu_{Rx}k_{Lz}}\right)\sin\left(k_{Lz}d_L\right)\sin\left(k_{Rz}d_R\right). \end{aligned} \quad (7)$$

It is evident that this dispersion relation can also be used, when the RHM is anisotropic. Here, for simplicity, we choose the RHM layers to be isotropic. When the wave vectors and the thicknesses of layers satisfy the condition,

$$k_{Lz}d_L + k_{Rz}d_R = m\pi, (m \in integers) \quad (8)$$

the right hand part of equation (7) will be larger than (or equal to) unity, and the Bloch wave vector q may be imaginary, indicating a gap, which is the familiar Bragg condition.

For the TM mode case, we have the magnetic and electric field in one unit cell as,

$$\begin{aligned} H_{Ly} &= e^{ik_x x}\left(e^{ik_{Lz}z} + Ae^{-ik_{Lz}z}\right), \\ E_{Lx} &= \frac{k_{Lz}}{\omega\varepsilon_{Lx}} e^{ik_x x}\left(e^{ik_{Lz}z} - Ae^{-ik_{Lz}z}\right), \\ E_{Lz} &= \frac{-k_x}{\omega\varepsilon_{Lz}} e^{ik_x x}\left(e^{ik_{Lz}z} + Ae^{-ik_{Lz}z}\right), \end{aligned} \quad (9)$$

in the anisotropic LHM layer and

$$\begin{aligned} H_{Ry} &= e^{ik_x x}\left(e^{ik_{Rz}z} + Ae^{-ik_{Rz}z}\right), \\ E_{Rx} &= \frac{k_{Rz}}{\omega\varepsilon_{Rx}} e^{ik_x x}\left(e^{ik_{Rz}z} - Ae^{-ik_{Rz}z}\right), \\ E_{Rz} &= \frac{-k_x}{\omega\varepsilon_{Rz}} e^{ik_x x}\left(e^{ik_{Rz}z} + Ae^{-ik_{Rz}z}\right), \end{aligned} \quad (10)$$

$$T_{period} = T_L T_R = \begin{pmatrix} 1 & -\mu_{Lx} d_L \frac{\omega}{c} \\ \frac{\varepsilon_{Ly}\mu_{Lx}\frac{\omega^2}{c^2} - \frac{\mu_{Lx}}{\mu_{Lz}}k_x^2}{\mu_{Lx}} d_L \frac{c}{\omega} & 1 \end{pmatrix} \begin{pmatrix} 1 & -\mu_{Rx} d_R \frac{\omega}{c} \\ \frac{\varepsilon_{Ry}\mu_{Rx}\frac{\omega^2}{c^2} - \frac{\mu_{Rx}}{\mu_{Rz}}k_x^2}{\mu_{Rx}} d_R \frac{c}{\omega} & 1 \end{pmatrix}$$
$$= \begin{pmatrix} 1 & -(\mu_{Lx} f_L + \mu_{Rx} f_R) d \frac{\omega}{c} \\ ((\varepsilon_{Ly} f_L + \varepsilon_{Ry} f_R)\frac{\omega^2}{c^2} - (\frac{f_L}{\mu_{Lz}} + \frac{f_R}{\mu_{Rz}})k_x^2) d \frac{c}{\omega} & 1 \end{pmatrix}, \quad (14)$$

in the isotropic RHM layer. The wave vector k_{Lz} can be determined as follows,

$$k_{L,Rz}^2 = \mu_{L,Ry}\varepsilon_{L,Rx}\frac{\omega^2}{c^2} - \frac{\varepsilon_{L,Rx}}{\varepsilon_{L,Rz}}k_x^2. \quad (11)$$

Similar with the above derivation in the TE case, the dispersion relation for the TM mode wave is,

$$\cos(qd) = \cos(k_{Lz}d_L)\cos(k_{Rz}d_R) - \frac{1}{2}\left(\frac{\varepsilon_{Rx}k_{Lz}}{\varepsilon_{Lx}k_{Rz}} + \frac{\varepsilon_{Lx}k_{Rz}}{\varepsilon_{Rx}k_{Lz}}\right)\sin(k_{Lz}d_L)\sin(k_{Rz}d_R), \quad (12)$$

and the Bragg condition also exists for the TM mode case.

2.2 Effective medium theory (EMT)

Since the negative refraction is realized in the GHz region, the product of the wave vector k_z and the thickness of one layer $d_{L,R}$ generally satisfy the condition $k_z d_{L,R} \ll 1$. In this regard, we can use the thin film approximation to analyze the $m = 0$ Bragg gap. The transfer matrices of the LHM layers and the RHM layers are as follows [12],

$$T_L = \begin{pmatrix} \cos(k_{Lz}d_L) & -\frac{\mu_{Lx}\omega}{k_{Lz}c}\sin(k_{Lz}d_L) \\ \frac{k_{Lz}c}{\mu_{Lx}\omega}\sin(k_{Lz}d_L) & \cos(k_{Lz}d_L) \end{pmatrix},$$
$$T_R = \begin{pmatrix} \cos(k_{Rz}d_R) & -\frac{\mu_{Rx}\omega}{k_{Rz}c}\sin(k_{Rz}d_R) \\ \frac{k_{Rz}c}{\mu_{Rx}\omega}\sin(k_{Rz}d_R) & \cos(k_{Rz}d_R) \end{pmatrix}, \quad (13)$$

for the TE mode case. Since $k_z d \ll 1$, we have $\sin(k_z d_{L,R}) \approx k_z d_{L,R}$, and $\cos(k_z d_{L,R}) \approx 1$ [18]. Then, the transfer matrix of a unit cell has the form,

(See equation (14) above)

in which, $f_L = d_L/d$, $f_R = d_R/d$. Because the photonic crystal composed of both isotropic materials can be effectively seen as a uniaxial material (with x,y-elements equal), in present paper, we can assume the effective electric permittivity and magnetic permeability tensors of the one-dimensional photonic crystal consists anisotropic LHM and isotropic RHM to be diagonalizable with the forms as [19],

$$\bar{\bar{\varepsilon}}_{eff} = \begin{pmatrix} \varepsilon_{effx} & 0 & 0 \\ 0 & \varepsilon_{effy} & 0 \\ 0 & 0 & \varepsilon_{effz} \end{pmatrix},$$
$$\bar{\bar{\mu}}_{eff} = \begin{pmatrix} \mu_{effx} & 0 & 0 \\ 0 & \mu_{effy} & 0 \\ 0 & 0 & \mu_{effz} \end{pmatrix}, \quad (15)$$

in which, the x, y-elements in the two tensors may not equal. Similar as equation (4), the effective wave vector k_z can be determined by the following equation,

$$k_{effz}^2 = \varepsilon_{effy}\mu_{effx}\frac{\omega^2}{c^2} - \frac{\mu_{effx}}{\mu_{effz}}k_{effx}^2, \quad (16)$$

and the effective transfer matrix of a period is:

$$T_{eff} = \begin{pmatrix} 1 & -\mu_{effx} d \frac{\omega}{c} \\ (\varepsilon_{effy}\frac{\omega^2}{c^2} - \frac{k_x^2}{\mu_{effz}}) d \frac{c}{\omega} & 1 \end{pmatrix}. \quad (17)$$

Comparing equations (14) with (17), we can easily give ε_{effy}, μ_{effx} and μ_{effz} as,

$$\mu_{effx} = \mu_{Lx} f_L + \mu_{Rx} f_R, \quad \varepsilon_{effy} = \varepsilon_{Ly} f_L + \varepsilon_{Ry} f_R,$$
$$\mu_{effz} = \mu_{Lz}\mu_{Rz}/(\mu_{Lz} f_R + \mu_{Rz} f_L). \quad (18)$$

This result can be indeed used, when both components are anisotropic. In our model, the RHM layers are isotropic, so that $\mu_{Rx} = \mu_{Rz} = \mu_R$, $\varepsilon_{Ry} = \varepsilon_R$. Here, we would like to mention that equation (18) can also be derived from the Bloch theorem, i.e. equation (7), if we take both $\cos(k_z d_{L,R})$ and $\sin(k_z d_{L,R})$ up to the second order, that is $\cos(k_z d_{L,R}) = 1 - \frac{1}{2}k_z^2 d_{L,R}^2$, $\sin(k_z d_{L,R}) = k_z d_{L,R}$.

On the other hand, for TM case, similarly, we have,

$$\varepsilon_{effx} = \varepsilon_{Lx} f_L + \varepsilon_{Rx} f_R, \mu_{effy} = \mu_{Ly} f_L + \mu_{Ry} f_R,$$
$$\varepsilon_{effz} = \varepsilon_{Lz}\varepsilon_{Rz}/(\varepsilon_{Lz} f_R + \varepsilon_{Rz} f_L), \quad (19)$$

and the effective wave vector k_{effz},

$$k_{effz}^2 = \mu_{effy}\varepsilon_{effx}\frac{\omega^2}{c^2} - \frac{\varepsilon_{effx}}{\varepsilon_{effz}}k_x^2. \quad (20)$$

The equation (19) can also be used, when both components are anisotropic. Since the RHM layers is isotropic, we have $\varepsilon_{Rx} = \varepsilon_{Rz} = \varepsilon_R$, $\mu_{Ry} = \mu_R$.

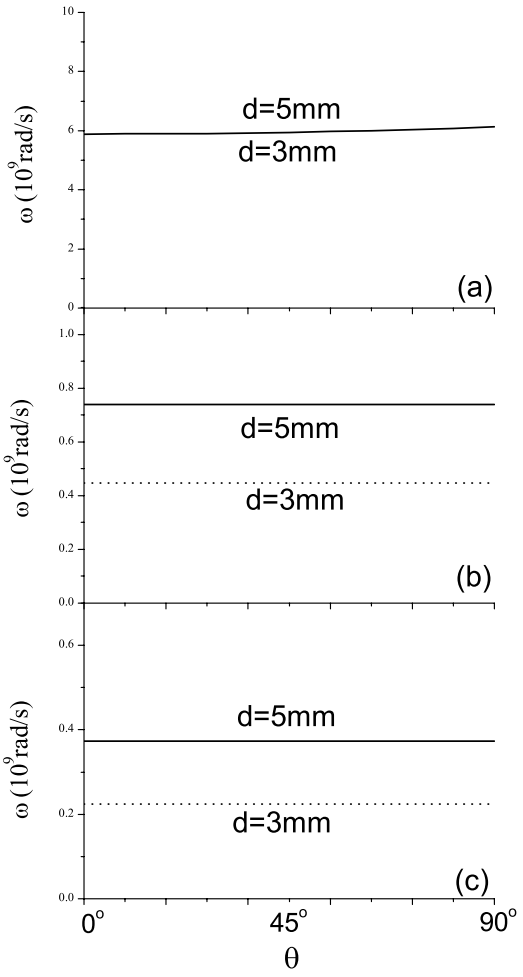

Fig. 1. The solutions of equation (5), with the incident angle changing from 0° to 90°, for (a) $m = 0$, (b) $m = -1$, (c) $m = -2$. Note that in (a) the curve for $d = 3$ mm and that for $d = 5$ mm overlap.

3 TE mode wave

3.1 Case I

In this case, we choose $\mu_{Lx} = 1 - 100/\omega^2$, $\varepsilon_{Ly} = 1 - 200/\omega^2$, $\mu_{Lz} = 2$. The similar forms as μ_{Lx} and ε_{Ly} chosen in present paper has been experimentally realized and theoretically used in previous reports [4,12,21]. Another reason to choose this simple forms of permittivity and permeability lies in the simplicity for comparing between the values of the effective permittivity and permeability. The permittivity and permeability of the isotropic RHM layer are chosen to be $\varepsilon_R = 3$, $\mu_R = 3$. From the forms of μ_{Lx} and ε_{Ly}, it is evident that in the angular frequency region $(0, 10\times10^9\,\mathrm{rad/s})$, μ_{Lx} and ε_{Ly} are simultaneously negative, resulting in the negative refraction in the anisotropic LHM. Therefore, we only need to concentrate on the transmission properties of the one-dimensional photonic crystal in this frequency region.

In Figure 1, the solutions of equation (8) are shown. Here, we choose the thicknesses of unit cell to be 10 mm, with one LHM layer and one RHM layer to be both 5 mm. Since, the solutions for m equal to positive integers correspond to the angular frequencies far away from the region $(0, 10\times10^9\,\mathrm{rad/s})$, so that they are not plotted in the figure. To one's interest, we find that the Bragg gaps keep almost invariant, with the incident angle changing from 0° to 90°. This indicates that these gaps may present omnidirectional reflection. However, after scaling the thicknesses of the layers to 3/5, we find that only the $m = 0$ Bragg gap remains still, while others move significantly. This phenomenon is quite similar with the $\bar{n} = 0$ gap in the one-dimensional photonic crystal containing both isotropic materials [11]. This special property of the $m = 0$ Bragg gap may be much useful in the designing of omnidirectional microwave mirrors. Therefore, in the following content, we will focus our attention only on the $m = 0$ Bragg gap. (Actually, the Bragg gaps for m equal to negative integers won't move significantly when the incident angles changes, but these gaps are rather narrow, which limits the practical applications.)

The transmission spectra for the TE wave with different incident angles are shown in Figure 2. We can see an ODR region exists in the $m = 0$ Bragg gap. Here, we give the theoretical interpretation of the existence of the ODR region. See in equation (16), if $\varepsilon_{effy} < 0$, $\mu_{effx} > 0$ and $\mu_{effz} > 0$, the factors of $\frac{\omega^2}{c^2}$ and k^2_{effx} are both negative, resulting k^2_{effz} to be always negative, so that k_{effz} is imaginary and the TE mode wave can not propagate in the periodic structure for all real k_x. This condition is called the always-cutoff condition [20]. In Figure 2, two dash lines correspond to two critical frequencies of $\omega^{TE}_{\varepsilon y}$ ($\varepsilon_{effy} = 0$) and $\omega^{TE}_{\mu x}$ ($\mu_{effx} = 0$), which divide the region $(0, 10\times10^9\,\mathrm{rad/s})$ into three parts **A**, **B**, **C**. The ODR region is just in the part **A**, in which $\varepsilon_{effy} < 0$, $\mu_{effx} > 0$ and $\mu_{effz} > 0$, satisfying the always-cutoff condition. In part **B**, the effective coefficients satisfy the condition of $\varepsilon_{effy} > 0$, $\mu_{effx} > 0$ and $\mu_{effz} > 0$, corresponding to the normal-cutoff condition, so that in Figure 2, when the incident angle turns larger, the lower frequency waves, with lower values of $\varepsilon_{effy}\mu_{effx}$, can not propagate in the structure. In region **C**, the effective coefficients satisfy $\varepsilon_{effy} < 0$, $\mu_{effx} < 0$ and $\mu_{effz} > 0$, corresponding to the never-cutoff condition, that is the wave can propagate in the periodic structure with all incident angles. Therefore, the edges of the ODR region can be determined by following conditions,

$$\omega^{TE}_{min}: \quad \varepsilon_{effy} = 0 \quad \text{and} \quad \omega^{TE}_{max}: \quad \mu_{effx} = 0. \tag{21}$$

Then, the exact value of the edges of the ODR region can be figured out as

$$\omega^{TE}_{min} = \omega^{TE}_{\mu x} = 5\times10^9\,\mathrm{rad/s} \quad \text{and} \quad \omega^{TE}_{max} = \omega^{TE}_{\varepsilon y} = 7.071\times10^9\,\mathrm{rad/s}. \tag{22}$$

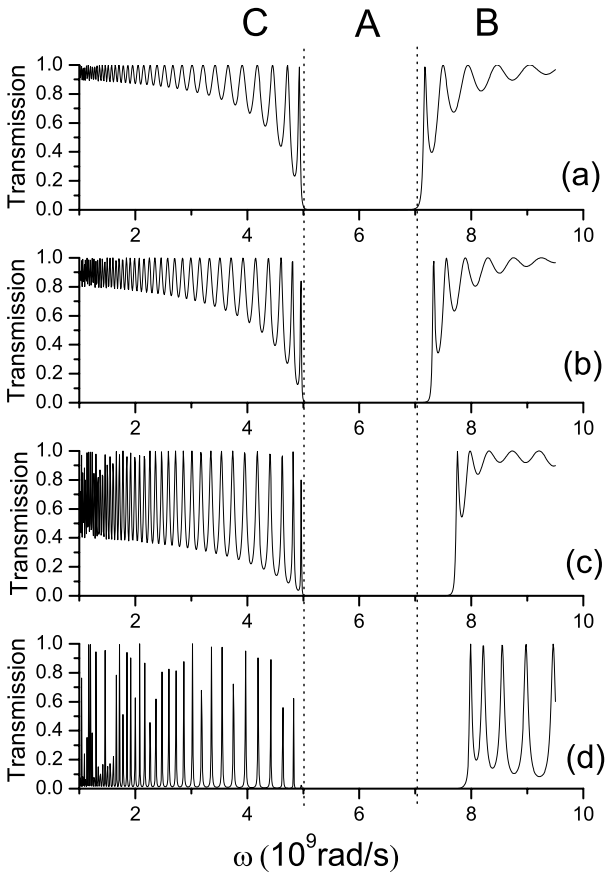

Fig. 2. The transmission for Case I of TE wave with different incident angles, (a) 0°, (b) 30°, (c) 60°, (d) 85°. The thickness of each layer is 5 mm, and the number of the unit cells is 60.

3.2 TE mode: case II

In case I, the parameters chosen correspond to the condition that $\omega_{\mu x}^{TE} < \omega_{\varepsilon y}^{TE}$. Here, in contrast to case I, we investigate the $m = 0$ Bragg gap with the condition that $\omega_{\mu x}^{TE} > \omega_{\varepsilon y}^{TE}$. For simplicity, we just exchange the forms of μ_{Lx} and ε_{Ly} to get $\mu_{Lx} = 1 - 200/\omega^2$, $\varepsilon_{Ly} = 1 - 100/\omega^2$, and other parameters remain the same as above. Since the similar result as Figure 1 can be easily found, we just focus our attention on the $m = 0$ Bragg gap to investigate the difference in transmission property between the two cases. The conditions $\mu_{eff\,x} = 0$ and $\varepsilon_{eff\,y} = 0$ determine the critical frequencies $\omega_{\mu x}^{TE}$ (7.071×10^9 rad/s) and $\omega_{\varepsilon y}^{TE}$ (5×10^9 rad/s), which divide the frequency spectrum into three parts **A**, **B** and **C** in Figure 3. In part **B** and part **C**, the transmission property and the cutoff condition remain the same as that in Case I, but in part **A**, we can see that the ODR region doesn't coincide with part **A**. With the incident angle increasing, the lower frequency waves begin to propagate in the periodic structure. This can be understood by using the results derived above. In part **A**, we have $\varepsilon_{eff\,y} > 0$, $\mu_{eff\,x} < 0$ and $\mu_{eff\,z} > 0$, substituting into equation (16), we find that with the incident angle increasing, k_x^2 increasing, too, as a result, $k_{eff\,z}^2$ may be positive when the value of $\mu_{eff\,x}\varepsilon_{eff\,y}$ is small, i.e. in the lower frequency region, which corresponds to the anti-cutoff condition [20]. So that the edges of ODR region can be easily determined,

$$\omega_{min}^{TE}: \quad \varepsilon_{eff\,y}\mu_{eff\,x} - \frac{\mu_{eff\,x}}{\mu_{eff\,z}} = 0 \quad \text{and} \quad \omega_{max}^{TE}: \quad \mu_{eff\,x} = 0, \tag{23}$$

and, here, ω_{min}^{TE} and ω_{max}^{TE} can be figured out to be 5.6195×10^9 rad/s and 7.071×10^9 rad/s, respectively.

In addition, by using the effective medium theory, we can predict that the ODR region won't be affected with a certain fluctuation of the thicknesses of the layers or undergoes scaling, as long as the condition $k_z d_{L,R} \ll 1$ is satisfied, which is shown in Figure 4. In the figure, for normal incidence, the profile of the case that the layer thickness equals 5 mm is almost the same as that of the thickness with fluctuation of 1/10, and the gaps for the three cases are almost the same.

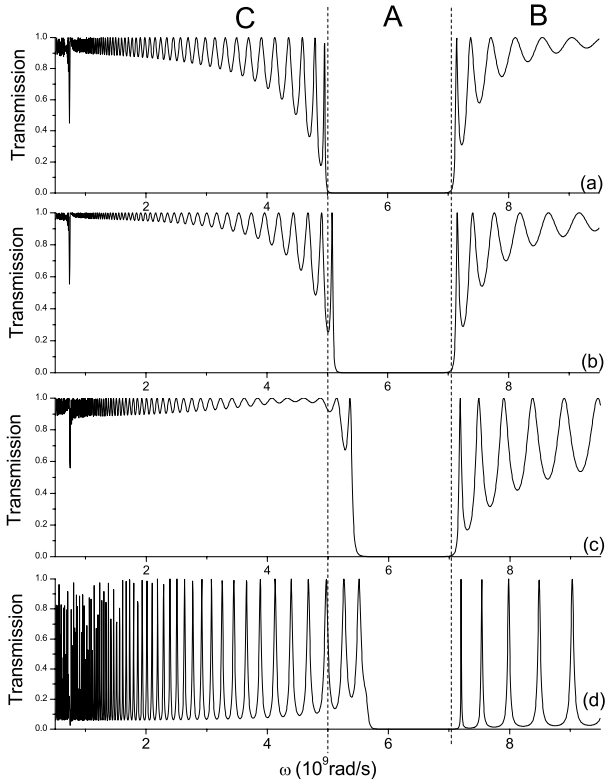

Fig. 3. The transmission for Case II of TE wave with different incident angles, (a) 0°, (b) 30°, (c) 60°, (d) 85°. Other parameters remain the same as above.

4 TM mode wave

4.1 Case I

For the TM mode case, we choose the parameters of the anisotropic LHM and the RHM as $\varepsilon_{Lx} = 1 - 100/\omega^2$, $\mu_{Ly} = 1 - 150/\omega^2$, $\varepsilon_{Lz} = 2$, and $\varepsilon_R = 3$, $\mu_R = 3$. The Bragg gaps for $m = 0, -1, -2$ are shown in Figure 5. Similar with the TE mode case, the Bragg gaps change very

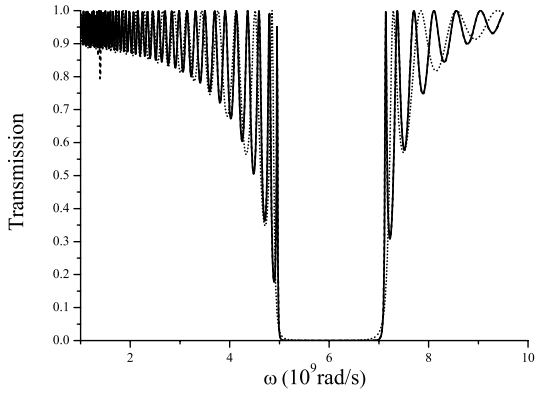

Fig. 4. The transmission for TE mode wave with the thicknesses of single layer are: (a) 5 mm (the solid line), (b) scaled by 3/5, i.e. 3 mm (the dotted line), (c) the thicknesses of the layers in the structure have a fluctuation of 1/10 (the dashed line).

slowly with the incident angle changing from 0° to 90°, and when the system undergoes scaling by 3/5, only the $m = 0$ Bragg gap keep invariant. Therefore, here we also focus our attention on the $m = 0$ Bragg gap. The transmission spectra for the TM wave are shown in Figure 6. In the figure, we can see that there exists an ODR region around $(5 \times 10^9\,\text{rad/s}, 6 \times 10^9\,\text{rad/s})$. Two dash lines corresponding to the positions of $\omega_{\varepsilon x}^{TM}$ ($\varepsilon_{eff\,x} = 0$) and $\omega_{\mu y}^{TM}$ ($\mu_{eff\,y} = 0$) divide the region $(0, 10 \times 10^9\,\text{rad/s})$ into three parts **A**, **B**, **C**. In part **A**, we have $\varepsilon_{eff\,x} < 0$, $\mu_{eff\,y} > 0$, $\varepsilon_{eff\,z} > 0$ satisfying the always-cutoff condition for the TM wave [20]. In the part **B**, $\varepsilon_{eff\,x} > 0$, $\mu_{eff\,y} > 0$, $\varepsilon_{eff\,z} > 0$, corresponding to the normal-cutoff condition, and in the part **C**, $\varepsilon_{eff\,x} < 0$, $\mu_{eff\,y} < 0$, $\varepsilon_{eff\,z} > 0$, which satisfies the never-cutoff condition. So that the edges of the ODR region can be determined by the follow equations:

$$\omega_{min}^{TM} : \varepsilon_{eff\,x} = 0 \quad \text{and} \quad \omega_{max}^{TM} : \mu_{eff\,y} = 0. \tag{24}$$

From these equations, we can figure out the exact edges of the ODR region is $\omega_{min}^{TM} = \omega_{\varepsilon x}^{TM} = 5 \times 10^9\,\text{rad/s}$ and $\omega_{max}^{TM} = \omega_{\mu y}^{TM} = 6.12372 \times 10^9\,\text{rad/s}$.

4.2 Case II

In the above case, we have $\omega_{\varepsilon x}^{TM} < \omega_{\mu y}^{TM}$, in contrast, in this case, we will investigate the transmission property and cutoff condition in the $m = 0$ Bragg gap with the condition $\omega_{\varepsilon x}^{TM} > \omega_{\mu y}^{TM}$. Here, for simplicity, we also just exchange the forms of ε_{Lx} and μ_{Ly} and have $\mu_{Ly} = 1 - 100/\omega^2$ and $\varepsilon_{Lx} = 1 - 150/\omega^2$. Similarly, in Figure 7, since $\mu_{eff\,y}$ and $\varepsilon_{eff\,x}$ are simultaneously positive or negative in part **B** and part **C**, the transmission property and cutoff condition are the same as case I of TM mode. The only difference between these two cases lies in part **A**. We can see that with the incident angle increasing, the lower frequency waves begin to propagate in the periodic structure. This result is much the same as the case II of TE mode wave and the part **A** just corresponds to the anti-cutoff condition,

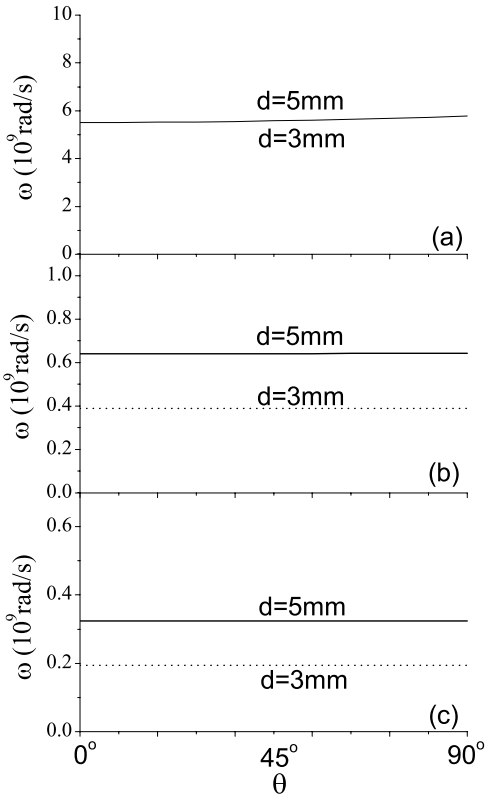

Fig. 5. The same as Figure 1 but for TM case.

so that the edges of the ODR region can be determined by these two equations.

$$\omega_{min}^{TM} : \quad \varepsilon_{eff\,x}\mu_{eff\,y} - \frac{\varepsilon_{eff\,x}}{\varepsilon_{eff\,z}} = 0 \quad \text{and} \quad \omega_{max}^{TM} : \quad \varepsilon_{eff\,x} = 0. \tag{25}$$

The ω_{min}^{TM} and ω_{max}^{TM} here is figured out to be $5.6195 \times 10^9\,\text{rad/s}$ and $6.12372 \times 10^9\,\text{rad/s}$.

We also investigate the cases of normal incidence for TM mode when the thicknesses of the layers undergo scaling or have certain rate of fluctuation, which is shown in Figure 8. Similar results with the TE mode case are obtained. The profile corresponding to the periodic structure with thickness fluctuation of 1/10 almost coincides with that of the periodic structure without thickness fluctuation and with the thicknesses of layers undergoes scaling, the gap also changes little.

5 Discussion and conclusion

To one's interest, we can get a complete reflection region (in this region, waves with all incident angles in both TE and TM mode can all be reflected) in this anisotropic one-dimensional photonic crystal with different forms of elements of the permittivity and permeability tensors, and the complete reflection region can be expressed as $\left[\omega_{min}^{TE}, \omega_{max}^{TE}\right] \cap \left[\omega_{min}^{TM}, \omega_{mam}^{TM}\right]$. If one carefully choose the elements' forms of the permittivity and permeability of

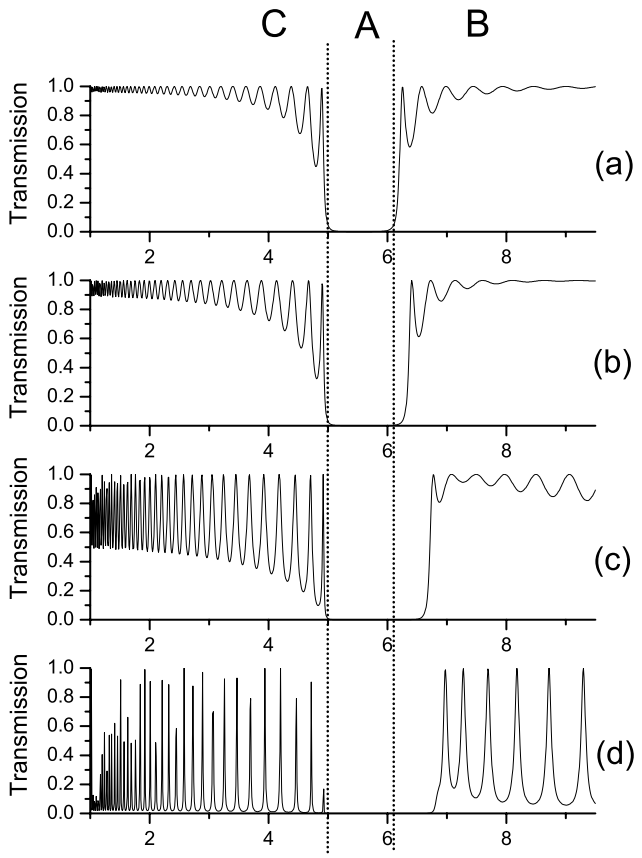

Fig. 6. The transmission for Case I of TM mode wave with different incident angles, (a) 0°, (b) 30°, (c) 60°, (d) 85°.

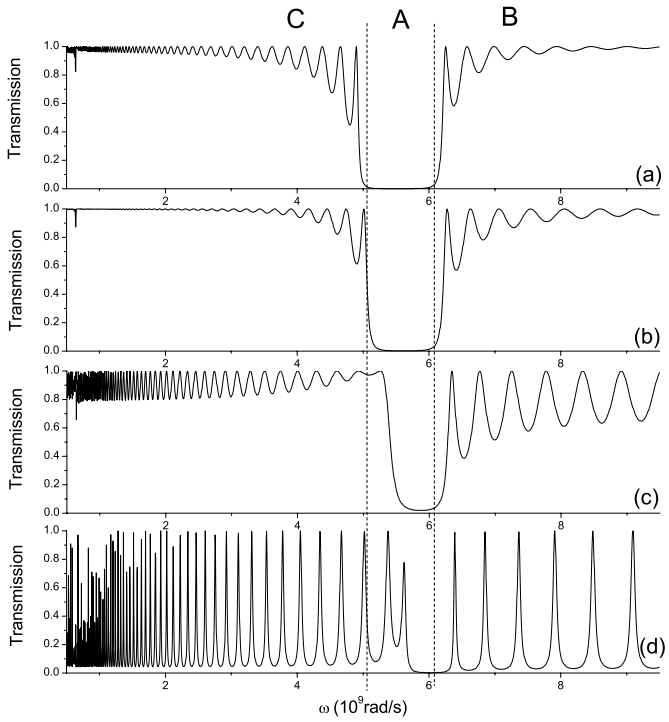

Fig. 7. The transmission for Case II of TM mode wave with different incident angles, (a) 0°, (b) 30°, (c) 60°, (d) 85°.

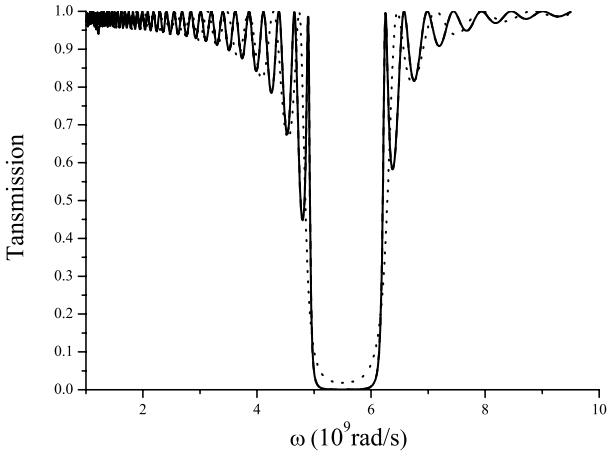

Fig. 8. The same as Figure 4 but for TM case.

the LHM, one can get a broad complete reflection region, which may be very useful in making microwave mirrors.

In fact, the elements of the anisotropic LHM layers can be chosen as other forms (uniaxial or bianisotropic). With different choosing of the elements of the permittivity tensor and the permeability tensor of the LHM layer, the results will be much different. For example, if we choose $\mu_{Lx} = \mu_{Ly} = \mu_{Lz}$ (for example, $1 - 100/\omega^2$), and $\varepsilon_{Lx} = \varepsilon_{Ly} = \varepsilon_{Lz}$ (for example, $1 - 200/\omega^2$), and other parameters remain the same as above, which is the case of the one-dimensional photonic crystal consists of isotropic LHM and RHM layers, the effective permittivity and permeability can also be determined as equations (18) and (19), but the effective material will be uniaxially anisotropic. For the TE mode wave, the case is similar with the case I in Section 3, and for the TM mode wave, the case is similar with the case II in Section 4. We can get a complete reflection region corresponding to $\left[\omega_{min}^{TE}, \omega_{max}^{TE}\right] \cap \left[\omega_{min}^{TM}, \omega_{max}^{TM}\right]$. However, with other choosing the forms of ε_L and μ_L, the complete reflection region in the $m = 0$ Bragg gap doesn't always exist for certain forms. As well as the cases considered in present paper to choose different forms of the elements of the anisotropic LHM to get complete reflection region, another practical method to get an optimal width of complete reflection region, one can carefully choose an anisotropic RHM with specific x, y, z-elements of permittivity tensor and permeability tensor to be one of the components in the one-dimensional photonic crystal, as well as a uniaxial LHM to be the other component.

In conclusion, we study the transmission properties and the dispersion relation of the one-dimensional photonic crystal containing alternate anisotropic left-handed material (LHM) layers and regular isotropic right-handed material (RHM) layers. The dispersion relation of an infinite periodic structure containing anisotropic LHM is derived, which to our knowledge is first reported. We find that there exists an ODR region in the $m = 0$ Bragg gap and this region is invariant for scaling, which is similar as the $\bar{n} = 0$ gap in isotropic one-dimensional photonic

crystal. By adopting the effective medium theory, we get the effective permittivity and permeability of the 1-D photonic crystal. We investigate the ODR region in the $m = 0$ Bragg gap for all cases of TE and TM mode with the aid of EMT method. Moreover, the edges of the ODR region are given out for all these cases, and the results predict a complete reflection region in the $m = 0$ Bragg gap.

It should be noted that, in the present paper, we only choose the x,y-elements of the permittivity and permeability of the LHM to be negative, and the z-element is chosen to be positive and dispersion-less. However, the z-element can also be negative, and the transmission property may be much more complicated, which need to be further studied.

This work was supported by the National Natural Science Foundation of China under Grant No. 10204017 and the Natural Science of Jiangsu Province under Grant No. BK2002038. The authors acknowledge the helps of Mr. C.J. Tang.

References

1. V.G. Veselago, Sov. Phys. Usp. **10** 509 (1968)
2. D.R. Smith, W.J. Padilla, D.C. Vier, S.C. Nemat-Nasser, S. Schultz, Phys. Rev. Lett. **84**, 4184 (2000)
3. D.R. Smith, N. Kroll, Phys. Rev. Lett. **85**, 2933 (2000)
4. J.B. Pendry, Phys. Rev. Lett. **85**, 3966 (2000)
5. N. Garcia, M. Nieto-Vesperinos, Phys. Rev. Lett. **88**, 207403 (2002)
6. J.B. Pendry, Phys. Rev. Lett. **91**, 099701 (2003)
7. Y. Fink, J.N. Winn, S. Fan, C. Chen, J. Michel, J.D. Joannopoulos, E.L. Thomas, Science **282**, 1679 (1998)
8. J.N. Winn, Y. Fink, S. Fan, J.D. Joannopoulos, Opt. Lett. **23**, 1573 (1998)
9. D.N. Chigrin, A.V. Larrinenko, D.A. Yarotsky, S.V. Gaponenko, Appl. Phys. A **68**, 25 (1999)
10. A. Mir, A. Akjouj, E.H. El Boudouti, B. Djafari-Ronhani, L. Dobrzynski, Vacuum **63**, 197 (2001)
11. Jensen Li, Lei Zhou, C.T. Chan, P. Sheng, Phys. Rev. Lett. **90**, 083901 (2003)
12. Haitao Jiang, Hong Chen, Hongqiang Li, Yewen Zhang, Shiyao Zhu, Appl. Phys. Lett. **83**, 5386 (2003)
13. Jing Li, Degang Zhao, Zhengyou Liu, Phys. Lett. A **332**, 461 (2004)
14. I. Abdulhalim, Opt. Commun. **174**, 43 (2000)
15. I. Abdulhalim, Opt. Commun. **215**, 225 (2003)
16. Zheng Liu, Jianjun Xu, Zhifang Lin, Opt. Commun. **240**, 19 (2004)
17. Liang Wu, Sailing He, Linfang Shen, Phys. Rev. B **67**, 235103 (2003); Zheng Liu, Liangbin Hu, Zhifang Lin, Phys. Lett. A **308**, 294 (2003)
18. A. Lakhtakia, C.M. Krowne, Optik **114**, 305 (2003); A.J. Abu El-Haija, J. Appl. Phys. **93**, 2590 (2003)
19. Masanori Abe, Manabu Gomi, Jpn. J. Appl. Phys. **23**, 1580 (1984)
20. D.R. Smith, D. Schuring, Phys. Rev. Lett. **90**, 077405 (2003)
21. G.V. Eleftheriades, A.K. Iyer, D.C. Kremer, IEEE Trans. Microwave Theory Tech. **50**, 2702 (2002)